

PCCP

Accepted Manuscript



This is an *Accepted Manuscript*, which has been through the Royal Society of Chemistry peer review process and has been accepted for publication.

Accepted Manuscripts are published online shortly after acceptance, before technical editing, formatting and proof reading. Using this free service, authors can make their results available to the community, in citable form, before we publish the edited article. We will replace this *Accepted Manuscript* with the edited and formatted *Advance Article* as soon as it is available.

You can find more information about *Accepted Manuscripts* in the [Information for Authors](#).

Please note that technical editing may introduce minor changes to the text and/or graphics, which may alter content. The journal's standard [Terms & Conditions](#) and the [Ethical guidelines](#) still apply. In no event shall the Royal Society of Chemistry be held responsible for any errors or omissions in this *Accepted Manuscript* or any consequences arising from the use of any information it contains.

Highly Active Electrolytes for Rechargeable Mg Batteries Based on [Mg₂(μ-Cl)₂]²⁺ Cation Complex in Dimethoxyethane

Yingwen Cheng,¹ Ryan M. Stolley,² Kee Sung Han,³ Yuyan Shao,¹ Bruce W. Arey³, Nancy M. Washton³, Karl T. Mueller,^{3,4} Monte L. Helm,² Vincent L. Sprenkle,¹
Jun Liu¹ and Guosheng Li^{1,*}

¹Energy Processes & Materials Division, Energy and Environmental Directorate, ²Catalysis Science Division, Fundamental & Computational Science Directorate, and ³Environmental Molecular Science Laboratory, Pacific Northwest National Laboratory, Richland, WA 99352, ⁴Department of Chemistry, Pennsylvania State University, University Park, PA 16802

Abstract: A novel [Mg₂(μ-Cl)₂]²⁺ cation complex, which is highly active for reversible Mg electrodeposition, was identified for the first time in this work. This complex was found to present in electrolytes formulated in dimethoxyethane (DME) through dehalodimerization of non-nucleophilic MgCl₂ by reacting with either Mg salts (such as Mg(TFSI)₂, TFSI= bis(trifluoromethane)sulfonylimide) or Lewis acid salts (such as AlEtCl₂ or AlCl₃). The molecular structure of the cation complex was characterized by single crystal X-ray diffraction, Raman spectroscopy and NMR. The electrolyte synthesis process was studied and rational approaches for formulating highly active electrolytes were proposed. Through control of the anions, electrolytes with efficiency close to 100%, wide electrochemical window (up to 3.5V) and high ionic conductivity (> 6 mS/cm) were obtained. The understandings of electrolyte synthesis in DME developed in this work could bring significant opportunities for rational formulation of electrolytes with the general formula [Mg₂(μ-Cl)₂][anion]_x for practical Mg batteries.

Introduction

Magnesium (Mg)-based rechargeable batteries have recently emerged as attractive candidates for the next generation energy storage due to the unique advantages of Mg metal.¹⁻³ Mg is an earth abundant and environmentally benign material and is safe to handle when used as anode, and has a low standard electrode potential and fast deposition/stripping kinetics without formation of dendritic structures.⁴ Over the past decades, significant progresses have been made in the quest for rechargeable Mg batteries, including the development of cathode materials,^{1, 5-8} electrolytes⁹⁻¹⁵, current collectors¹⁶⁻¹⁸ and anode materials.¹⁹⁻²¹ The commercialization of Mg batteries, however, has not yet been demonstrated and still faces great challenges. Substantial advances, particularly on the development of stable/safe electrolytes with wide electrochemical windows and on high voltage cathode materials with high capacity, are critically required.

The electrolyte is one key component for rechargeable batteries.^{22, 23} It provides electrochemically active species and determines the electrode-electrolyte interfaces both for cathode and anode electrochemical reactions, and therefore, plays pivotal roles in determining battery performance. The importance of electrolyte for Mg battery development is particularly significant and it is currently a major limiting factor for their practical applications.¹¹ Simple battery electrolytes prepared by dissolving Mg salts, such as $\text{Mg}(\text{ClO}_4)_2$, in aprotic solvents are usually not able to produce reversible Mg deposition, most likely due to formation of blocking layers.²⁴

During the past decades, there has been an increase in studies for formulating electrolytes capable of reversible Mg deposition.^{2, 11, 25, 26} Gregory et al. initially developed ethereal solutions containing Mg organo-aluminates or Mg organo-borates and examined their activities for Mg

deposition.²⁷ Aurbach et al. later demonstrated electrolytes with anodic stability of ~ 2.5 V through reacting Grignard reagents (MgR_2 , R=ethyl and butyl) with aluminum containing Lewis acids (AlEtCl_2 or AlCl_3) and established the first prototypes of rechargeable Mg batteries.¹ Since then this class of electrolyte has been intensively studied and its properties were further optimized using the same concept through proper combinations of different Mg Grignard reagents and Lewis acid compounds.²⁸ For example, Pour et al. used phenyl magnesium chloride and synthesized all-phenyl-complex (APC) electrolytes that have electrochemical windows exceed 3.3V.^{10, 29} Because of the inherent safety concerns related to Grignard reagents, other Mg compounds such as MgCl_2 ,¹³⁻¹⁵ ROMgCl ,³⁰ hexamethyldisilazide magnesium chloride (HDMSMgCl),³¹ and Magnesium bistrifluoromethane sulfonyl imide ($\text{Mg}[\text{TFSI}]_2$)^{32, 33} were recently used to formulate electrolytes. Interestingly, crystallographic studies suggest that the cation complex unit $[\text{Mg}_2(\mu\text{-Cl})_3]^+$ was commonly observed in almost all of the salts crystallized from electrochemically active magnesium organohaloaluminate and magnesium organoborate electrolytes in tetrahydrofuran (THF) solution. This cation complex consisted of two octahedrally coordinated Mg atoms bridged by three chloride atoms and paired with a counter anion.^{12, 13, 34} It should be noted, though, that in solution this complex might be in thermodynamic equilibrium with THF-solvated $\text{MgCl}_2/\text{MgCl}^+$ species and therefore the actual composition of the electrolyte is rather complicated.^{11, 14} Compared with these THF-based electrolytes that have been studied relatively well, formulation of electrolytes in other ethereal solvents (such as DME and diglyme) has been studied to a far lesser extent. Successful demonstration and fundamental understanding of the synthesis of electrolytes in solvents with better thermal and chemical stability than THF is critical for future improvements of feasible rechargeable Mg batteries.

In this paper we report the first identification and analysis of an unique active cation complex $[\text{Mg}_2(\mu\text{-Cl})_2(\text{DME})_4]^{2+}$ for reversible Mg deposition and discuss factors that could affect its activity. This complex was found to present in a series of electrolytes formulated in DME by dehalodimerization of MgCl_2 through reacting with either Mg salts ($\text{Mg}(\text{TFSI})_2$) or Lewis acid salts (AlEtCl_2 or AlCl_3) and the approach could be extended to other salt combinations. The chemical structure was studied and confirmed with single crystal X-ray diffraction (XRD), Raman spectroscopy and ^{25}Mg and ^{27}Al nuclear magnetic resonance (NMR). Furthermore, it was found that through the control of anion chemistry (both type and concentration), electrolytes with coulombic efficiency close to 100%, high anodic stability (~ 3.5 V), and high ionic conductivity (~ 6 mS/cm) could be obtained readily. Our results suggest that solvent molecules play critical roles in determining the structure of active Mg species and strongly affect their activity for Mg deposition. The electrolyte synthesis and understandings developed in this work could be insightful for rational formulation of a family of electrolytes with the general formula $[\text{Mg}_2(\mu\text{-Cl})_2(\text{DME})_4][\text{anion}]_x$, and provide new opportunities for developing cathode materials, and therefore could be significant for practical Mg batteries.

Results and Discussion:

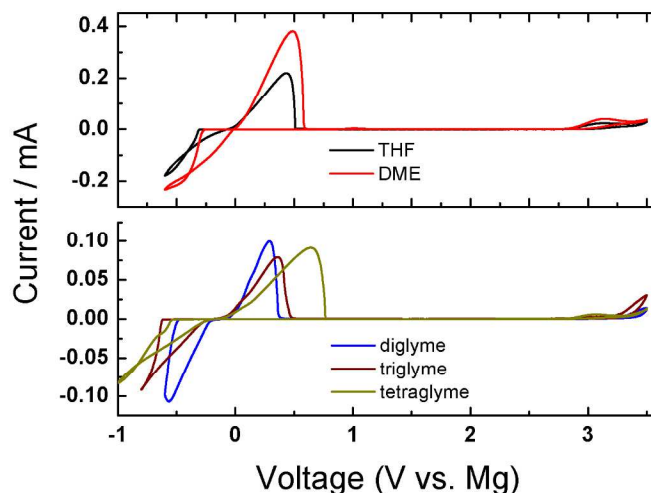


Figure 1: CVs (2nd cycle) of Mg electrolytes synthesized by reacting 0.4M MgCl₂ with desired amount of AlEtCl₂ (see Table 1 for details) in different solvents as indicated. Note that all of these electrolytes were able to produce reversible Mg deposition and stripping. The electrochemical properties of these electrolytes are summarized in Table 1.

Our previous work demonstrated synthesis of active Mg electrolytes by reacting MgCl₂ with Lewis acids in THF.¹³ The use of THF, however, could be problematic for practical applications because it has low boiling point (66°C) and flash point (-14°C). This intrinsic property of THF has motivated us to study formulation of Mg electrolytes in ethereal solutions with better thermal and chemical stability. To do this, we started with synthesis of electrolyte solutions in DME, diglyme, triglyme and tetraglyme using identical concentrations of precursors (0.4M MgCl₂ and 0.4M AlEtCl₂). The reaction products, without any purification, were directly used to examine their activity for Mg plating and stripping. Figure 1 shows a set of CVs recorded from these solutions at 20 mV/s on Pt working electrode and Table 1 provides a comparison of their electrochemical activities (Mg deposition overpotential, coulombic efficiency) and ionic conductivity. The behavior of typical MgCl₂-AlEtCl₂/THF electrolytes was also provided for reference.¹³ It was found that all of these electrolytes were able to produce reversible Mg deposition and stripping and they exhibited similar anodic stability. A small irreversible

oxidization peak at ca. ~ 2.9 V vs. Mg, presumably due to reactions of AlEtCl_4^- anions, was observed for all these electrolytes and is limiting the anodic stability.¹³ However, it should be noted that the anodic stability could be extended through optimization of anion chemistry using approaches, for example, that have been established for THF-based electrolytes.^{14,15} More importantly, these electrolyte solutions showed pronounced solvent dependent electroactivity for Mg deposition (Table 1), likely due to the differences of solvent Mg ion complex structures with chloride ions and different solvent molecules, which in turn have difference physicochemical properties in solvent, such as mobility, chemical stability and reactivity. Overall, the comparison implies that the electrolyte formulated in DME has beneficial properties for Mg deposition and has a high cycling efficiency (at least 95%, stable), a high ionic conductivity (4.10 mS/cm), low Mg deposition overpotential (220 mV) and high Mg deposition current density (Figure 1). The high ionic conductivity is similar to the well-established all-phenyl-complexes based electrolytes.²⁶ Therefore, all further experiments in this work were focused on this electrolyte system, but it should be noted that the properties of electrolytes synthesized in other long-chain glymes are also encouraging and worth further investigation.

Table 1: Electrochemical properties of electrolytes synthesized using 0.4 M MgCl_2 and desired amount of AlEtCl_2 in different solvents as indicated. These data was obtained based on CV experiments with Pt working electrodes (1mm) at 20 mV/s.

| Solvent | Overpotential for Mg deposition (mV) | Coulombic efficiency (%) | Ionic conductivity (mS/cm) |
|---|--------------------------------------|--------------------------|----------------------------|
| 3:2 MgCl_2 - AlEtCl_2 /THF | 252 | 95% | 2.09 |
| 1:1 MgCl_2 - AlEtCl_2 /DME | 220 | 95% | 4.10 |
| 1:1 MgCl_2 - AlEtCl_2 /diglyme | 404 | 81% | 2.29 |
| 1:1 MgCl_2 - AlEtCl_2 /triglyme | 466 | 86% | 1.19 |
| 1:1 MgCl_2 - AlEtCl_2 /tetraglyme | 384 | 84% | 0.95 |

The outstanding activity for electrolytes synthesized in DME is particularly attractive and was therefore further studied. The structure of the active species presented in this electrolyte was first analyzed using single crystal X-ray diffraction. The solid crystals were prepared by layering

hexane on the top of 3 ml $\text{MgCl}_2\text{-AlEtCl}_2/\text{DME}$ electrolyte and were identified as having the ionic pair of $[\text{Mg}_2(\mu\text{-Cl})_2(\text{DME})_4][\text{AlEtCl}_3]_2$ (Figure 2a and Table S1-S6). The cation complex consists of two octahedrally coordinated Mg centers bridged by two chlorine atoms. The four remaining sites on each Mg atom are coordinated through the oxygen atoms provided by two DME molecules. The anion is an aluminum atom tetrahedrally coordinated by one ethyl group and three chlorine atoms. This complex has fundamentally different molecular structure comparing to the $[\text{Mg}_2(\mu\text{-Cl})_3(\text{THF})_6]^+$ complex observed in THF-based electrolyte,^{2, 13} and could provide new opportunities for rational formulation of Mg electrolytes. In addition to the $\text{MgCl}_2\text{-AlEtCl}_2$ combination, we also confirmed that electrolytes synthesized in DME using $\text{MgCl}_2\text{-AlCl}_3$ and $\text{MgCl}_2\text{-Mg}(\text{TFSI})_2$ also have the same cation species (Figure 3b, Table S7-S12, and discussions below). We note that recent works reported synthesis of electrolytes in DME using similar formulas, $\text{MgCl}_2/\text{AlCl}_3$ and $\text{MgCl}_2/\text{Mg}(\text{TFSI})_2$, but the structure of the active species was not identified,^{15, 32} and this present study represent as the first identification of this active species.

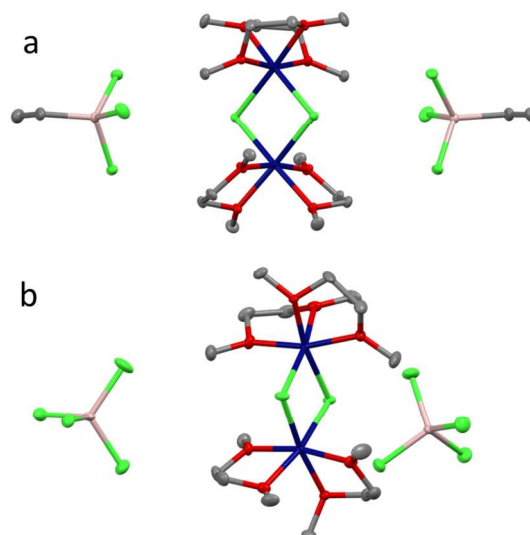


Figure 2: Molecular structures of (a) $[\text{Mg}_2(\mu\text{-Cl})_2(\text{DME})_4][\text{AlEtCl}_3]_2$ and (b) $[\text{Mg}_2(\mu\text{-Cl})_2(\text{DME})_4][\text{AlCl}_4]_2$. Mg atoms are shown in blue, Cl atoms in green, O atoms in red, Al atoms in ivory, and carbon atoms in grey. OLEX plot at 30% thermal probability ellipsoids. Hydrogen atoms are not shown for clarity. Molecular structures of (a) $[\text{Mg}_2(\mu\text{-Cl})_2(\text{DME})_4][\text{AlEtCl}_3]_2$ and (b) $[\text{Mg}_2(\mu\text{-Cl})_2(\text{DME})_4][\text{AlCl}_4]_2$ (Mg Blue, Cl green, Al, grey; C, color). OLEX plot at 30% thermal probability ellipsoids. Hydrogen atoms are not shown for clarity. Pertinent bond angles and lengths for a): Cl(1)-Mg(1)-Cl(2): 89.24° , Cl(1)-Mg(2)-Cl(2): 88.46° , Mg(1)-Cl(1) and Mg(1)-Cl(2): 2.446 \AA , Mg(2)-Cl(1) and Mg(2)-Cl(2): 2.463 \AA . Mg(1)-O bonds have identical lengths of 2.096 \AA , Mg(2)-O_{equatorial}: 2.112 \AA , Mg(2)-O_{axial}: 2.075 \AA , Al-C(11): 1.970 \AA , Al-Cl average bond length of 2.125 \AA . Pertinent bond angles and lengths for b): Cl(1)-Mg(1)-Cl(2): 88.00° , Cl(1)-Mg(2)-Cl(2): 87.41° , Mg(1)-Cl(1): 2.425 \AA , Mg(1)-Cl(2): 2.456 \AA , Mg(2)-Cl(1): 2.472 \AA , Mg(2)-Cl(2): 2.435 \AA . Mg(1)-O average length of 2.099 \AA , Mg(2)-O(7): 2.112 \AA , Mg(2)-O(6) 2.101 \AA , Al-Cl average bond length of 2.131 \AA .

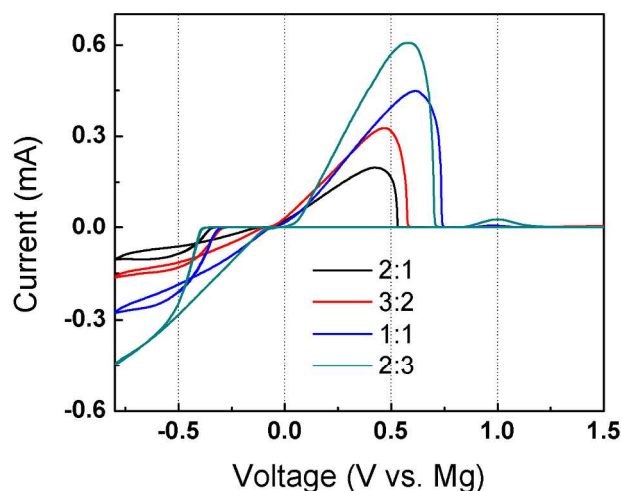


Figure 3: CV (2nd cycle) of 0.4M MgCl₂ electrolyte solutions synthesized in DME with different ratios of AlEtCl₂ as indicated (the ratios refer to the molar ratio between MgCl₂ and AlEtCl₂). These data were measured on 1 mm Pt working electrode at a scan rate of 20 mV/s.

The composition of solid crystals suggests the possible reaction involved in the synthesis of electrolytes is $\text{MgCl}_2 + \text{AlEtCl}_2 \rightarrow [\text{Mg}_2(\mu\text{-Cl})_2(\text{DME})_4][\text{AlEtCl}_3]_2$ in DME. To gain more insight on this reaction, we synthesized and analyzed a series of solutions using 0.4M MgCl₂ and varied concentration of AlEtCl₂. It should be noted that the stoichiometry of the proposed reaction suggests 0.4M AlEtCl₂ is required for completed reaction. All of the as-synthesized electrolytes were transparent and have no precipitates, and were directly used for electrochemical studies. Figure 3 shows a set of CVs obtained with a Pt electrode at 20 mV/s, and Table 2 compares their activities for Mg deposition and ionic conductivity. It was observed that the electrochemical properties of these electrolytes had strong dependence on the precursor ratios. In particular, both the ionic conductivity and Mg deposition current density increased noticeable with the increases of AlEtCl₂ concentration. The solutions synthesized with low concentrations of AlEtCl₂ ($\leq 0.4\text{M}$) had similar overpotential (~ 200 mV) and coulombic efficiency ($\sim 95\%$) for Mg deposition whereas the solution with excess AlEtCl₂ (0.6 M) had noticeably higher overpotential and lower coulombic efficiency. Additionally, a small anodic peak at ~ 1.0 V was

observed when the concentration of AlEtCl_2 exceeds 0.4M and will be discussed below. If we assume the ionic species in this electrolyte were mostly $[\text{Mg}_2(\mu\text{-Cl})_2(\text{DME})_4]^{2+}$ cation and AlEtCl_3^- anion, the observed higher ionic conductivity and Mg deposition activity with the increased concentration of AlEtCl_2 suggest that more ionic species are generated. This assumption is reasonable because compared with the case in THF, formation of species such as MgCl^+ and Mg_2Cl_3^+ are not favored thermodynamically in DME due to difficulties in fulfilling a coordination number of 6.^{26, 35}

Table 2: Electrochemical properties of electrolytes synthesized using 0.4M MgCl₂ and desired AlEtCl₂ in different solvents as indicated. These data was obtained based on CV experiments with Pt working electrodes (1mm) at 20 mV/s.

| Solvent | Overpotential for Mg deposition (mV) | Coulombic efficiency (%) | Conductivity (mS/cm) |
|---|--------------------------------------|--------------------------|----------------------|
| 0.4M MgCl ₂ + 0.2M AlEtCl ₂ /DME | 216 | 95% | 2.10 |
| 0.4M MgCl ₂ + 0.27M AlEtCl ₂ /DME | 202 | 95% | 2.72 |
| 0.4M MgCl ₂ + 0.4M AlEtCl ₂ //DME | 220 | 95% | 3.90 |
| 0.4M MgCl ₂ + 0.6M AlEtCl ₂ //DME | 360 | 85% | 4.32 |
| 0.8M MgCl ₂ + 0.8M AlEtCl ₂ /DME | 209 | 95% | 6.72 |

To better explain the obtained data, we propose that the reaction for our experiments was under dynamic equilibrium and did not completely convert to the dimer species with stoichiometry precursors. Even though it is not clear what the limiting step for the reaction is, it is evident that increasing the concentration of AlEtCl₂ will drive the reaction and result in higher yields of the dimer cation. To gain more insight, we characterized these electrolytes using ²⁷Al NMR (Figure 4). The ²⁷Al NMR spectrum is very sensitive to the symmetry of the molecule and the nature of the ligands and therefore is a useful technique to identify Al species. Three main ²⁷Al resonances were observed from these electrolytes and they can be assigned based on results from standard solutions as well as from literature.^{26, 36} The peaks at chemical shifts of ~ 24.5 ppm and ~128 ppm can be assigned to the precursor compound AlEtCl₂.³⁷ The peak at ~ 103.0 ppm could be assigned to AlCl₄⁻,^{13, 35} which is believed to originate from ligand exchange of AlEtCl₂. The broad peak at ~ 127.9 ppm can be assigned to from AlEtCl₃⁻.³⁸ Among species presented, the resonance attributed to AlEtCl₂ (at 24.5 ppm) is particularly meaningful for understanding the reaction. When the ratio between MgCl₂ and AlEtCl₂ was 2:1 no residual AlEtCl₂ was observed. Trace amounts of this species were observed for the 1:1 combination and with a considerable amount present when the ratio was 1:1.5. These comparisons suggest that

with the 1:1 ratio the reaction will not go to completion and some unreacted AlEtCl_2 , as well as some solvated MgCl_2 , was still present in the solution. Excess MgCl_2 is needed for complete reaction of AlEtCl_2 and excess AlEtCl_2 will likewise be required for complete conversion of MgCl_2 to the dimer cation complex.

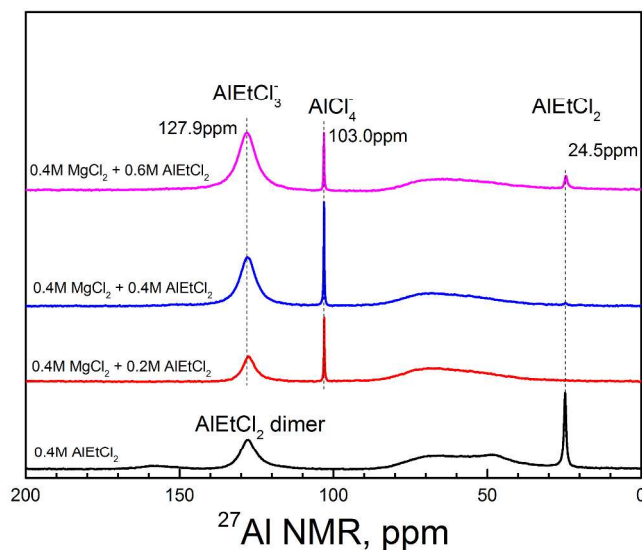


Figure 4: ^{27}Al NMR spectra of different solutions as indicated.

The electrochemistry and spectroscopy results confirm that the reaction between MgCl_2 and AlEtCl_2 will not convert to the dimer cation complex completely and the degree of conversion will be thermodynamically limited even at elevated temperature (60°C as used in this study). This fact is important for understanding the properties of electrolytes, as the species present in the electrolyte could have pronounced effects on the cycling behavior of batteries. For example, the solution with excess AlEtCl_2 (0.6M, Table 2) exhibited a noticeably higher overpotential and a lower coulombic efficiency along with a small cathodic peak at $\sim 1.0\text{V}$. This peak is at position similar with the oxidization of Al metal and therefore suggest formation of Al species in this electrolyte.¹⁶ These results imply that residual AlEtCl_2 could substantially affect

the electrochemical activity and stability of the electrolyte and its concentration should be minimized through controlling the concentration of MgCl_2 .

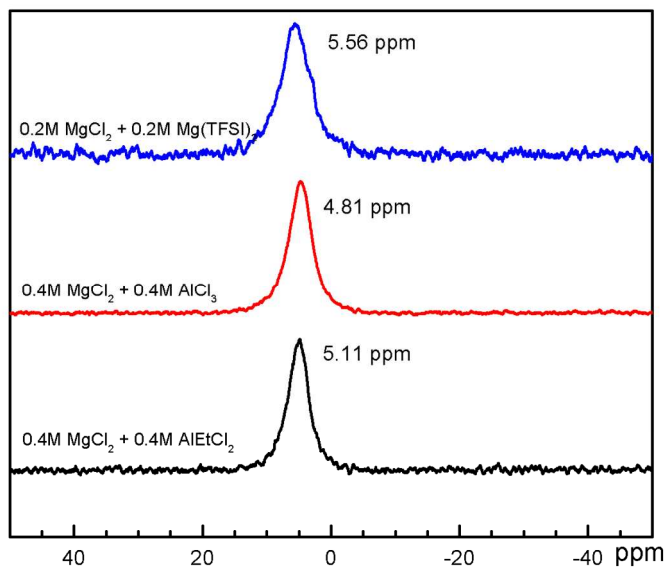


Figure 5: ^{25}Mg NMR spectra of different electrolytes synthesized in DME.

The above results clearly suggest that the dimer $[\text{Mg}_2(\mu\text{-Cl})_2(\text{DME})_4]^{2+}$ complex is present in electrolytes synthesized using MgCl_2 - AlEtCl_2 in DME, and it is logical to study whether this complex is generally present in DME-based electrolytes. To address this question, we synthesized and analyzed two additional set of solutions by reacting 0.4M MgCl_2 with either 0.4M AlCl_3 or 0.4M $\text{Mg}(\text{TFSI})_2$ in DME. Single crystal XRD analysis performed on the MgCl_2 - AlCl_3 /DME electrolyte revealed that the ionic pair was indeed $[\text{Mg}_2(\mu\text{-Cl})_2(\text{DME})_4][\text{AlCl}_4]_2$ (Figure 2b, Table S7-S12). We then performed ^{25}Mg NMR analysis on these three solutions, since multinuclear NMR spectroscopy has been demonstrated as a suitable technique for analyzing the chemical structure of complex Mg electrolyte solutions.^{26, 35} Chemical shifts of Mg ions for these three electrolytes were similar and were all around ~ 5 ppm (Figure 5). Given the high sensitivity of Mg chemical shift on chemical environment, we believe that the same cation complex was formed in each of these electrolytes.

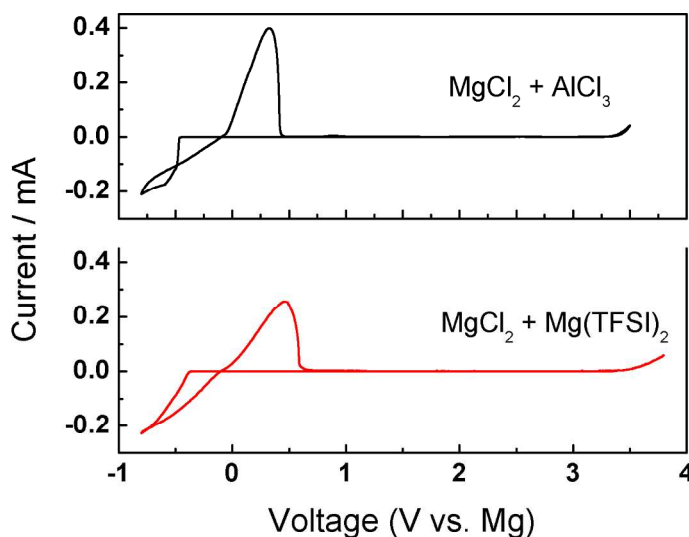
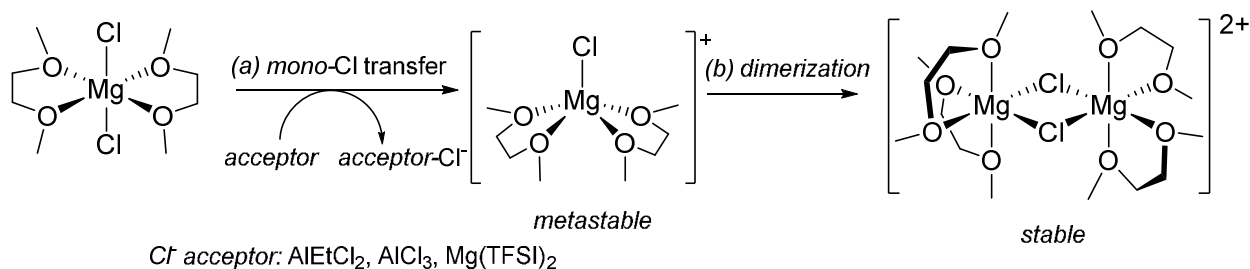


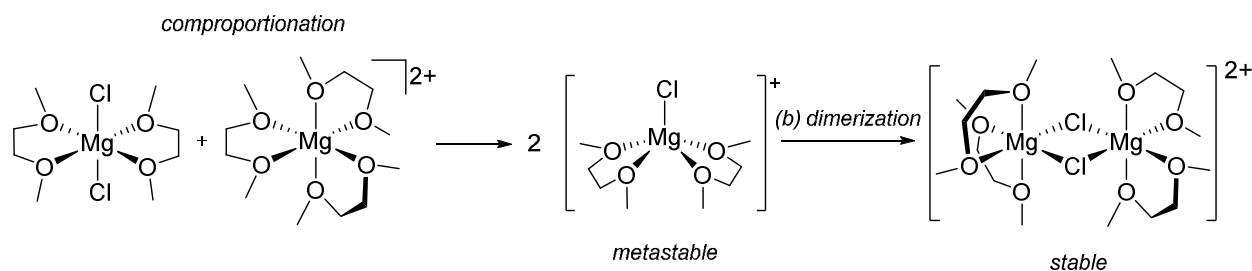
Figure 6: CV (2nd cycle) of electrolytes synthesized in DME by reacting 0.4M MgCl_2 with 0.4M AlCl_3 or 0.4M $\text{Mg}(\text{TFSI})_2$ as indicated, measured on Pt working electrode at a scan rate of 20 mV/s.

Figure 6 compares the electrochemical activities of these two electrolytes (see Figure 1 and 3 for MgCl_2 - AlEtCl_2 /DME electrolytes). It was found that both of them had good activity for Mg deposition/dissolution, and electrochemical windows wider than the MgCl_2 - AlEtCl_2 /DME electrolyte due to differences in anions. The MgCl_2 - AlCl_3 /DME electrolyte had an overpotential of ~ 200 mV, coulombic efficiency of 95% and anodic stability of ~ 3.4 V, whereas the MgCl_2 - $\text{Mg}(\text{TFSI})_2$ /DME electrolyte had an overpotential of ~ 400 mV, efficiency of $\sim 80\%$ and anodic stability of ~ 3.5 V. The comparison of these results with the MgCl_2 - AlEtCl_2 /DME electrolyte suggests that chemistry of anions has strong influences on the behavior of electrolytes. It should be noted, though, that other factors (such as impurities and precursor compound ratios) might also contribute to the differences in the measured performance results. Further studies on mechanistic understanding of these electrolytes consist of $[\text{Mg}_2(\mu\text{-Cl})_2(\text{DME})_4]$ using approaches similar with the studying of the MgCl_2 - AlEtCl_2 /DME electrolyte could further optimize their activities for Mg deposition.



Scheme 1: Proposed reaction path to $[\text{Mg}_2(\mu\text{-Cl})_2\text{DME}_4]^{2+}$ via *mono*-Cl transfer

On the basis of the above results, the pathways for electrolyte synthesis in DME were rationalized as dehalodimerization of MgCl_2 and are shown in Scheme 1 and 2. The dehalodimerization process involves the *mono*-Cl transfer from MgCl_2 to some chemical species that can be termed generally as chloride ion acceptors, and the overall reaction was driven thermodynamically by the ability of the acceptor to abstract one Cl^- off MgCl_2 and/or formation of the more stable dimer species. Overall, it has been recognized that solvated Mg^{2+} ion has a six-coordinated, octahedral structure. The structure of solvated MgCl_2 in THF has been reported as *trans*- $\text{MgCl}_2(\text{THF})_4$.¹³ In analogy with THF, we propose that the most feasible structure of solvated MgCl_2 in DME is *trans*- $\text{MgCl}_2(\text{DME})_2$ as shown in the scheme. During the reaction, one equivalent of *trans*- $\text{MgCl}_2(\text{DME})_2$ transfers one equivalent chloride ion to the acceptor through Cl transfer pathway. The chloride ion acceptor could be a Lewis acid compound, such as AlEtCl₂ and AlCl₃, or a Mg compound that is solvable in DME, such as Mg(TFSI)₂. The mechanism of *mono*-Cl transfer (reaction a) for the reaction of MgCl_2 and Lewis acid compound is straightforward as Lewis acid is strong electron acceptor. The chloride abstraction results in the formation of metastable of $[\text{MgCl}(\text{DME})_2]^+$ cation, which then undergoes a self-dimerization process (reaction b) to form thermodynamically more stable $[\text{Mg}_2(\mu\text{-Cl})_2(\text{DME})_4]^{2+}$ dimer cation.



Scheme 2: Proposed reaction path to $[\text{Mg}_2(\mu\text{-Cl})_2\text{DME}_4]^{2+}$ via comproportionation

The reaction of MgCl_2 and $\text{Mg}(\text{TFSI})_2$, however, is not as straightforward and can be understood as follows (Scheme 2). TFSI is a bulky non-coordinating anion and does not involve to the first coordination shell of DME-solvated Mg^{2+} , which should have the structure of $[\text{Mg}^{2+}(\text{DME})_3](\text{TFSI})_2$ based on ^{25}Mg NMR measurement (-0.94 ppm, Figure S1).³⁹ The stabilization of the highly charged cation $[\text{Mg}(\text{DME})_3]^{2+}$ from a strong anionic ligand, such as Cl^- , would be sufficient enough to abstract a Cl^- from the solvated MgCl_2 . This results in an overall *comproportionation* to again afford metastable $[\text{MgCl}(\text{DME})_2]^+$ cation from Cl^- transfer. After dimerization, it is possible that there is dynamic equilibrium between the species of $\text{MgCl}_2(\text{DME})_2$, $[\text{MgCl}(\text{DME})_2]^+$, and $[\text{Mg}_2(\mu\text{-Cl})_2(\text{DME})_4]^{2+}$ and their ratio is determined thermodynamically. In comparison with typical electrolytes synthesis in THF that involved transmetalation reaction between organomagnesium and Lewis acids that result in generation of complex mixture of species with various moieties,^{10, 40} the present synthesis is straightforward and cleaner with minimal side-reaction products. In fact, the comparison of the Raman spectra of the $[\text{Mg}_2(\mu\text{-Cl})_2(\text{DME})_4][\text{AlEtCl}_3]_2$ solid crystals and the electrolyte solutions reveals that no Mg-related peaks other than the dimer species was observed (Figure S2). The present clean electrolyte solutions with well-defined solution chemistry could have particular significance for the understanding and design of Mg cathode research.³¹

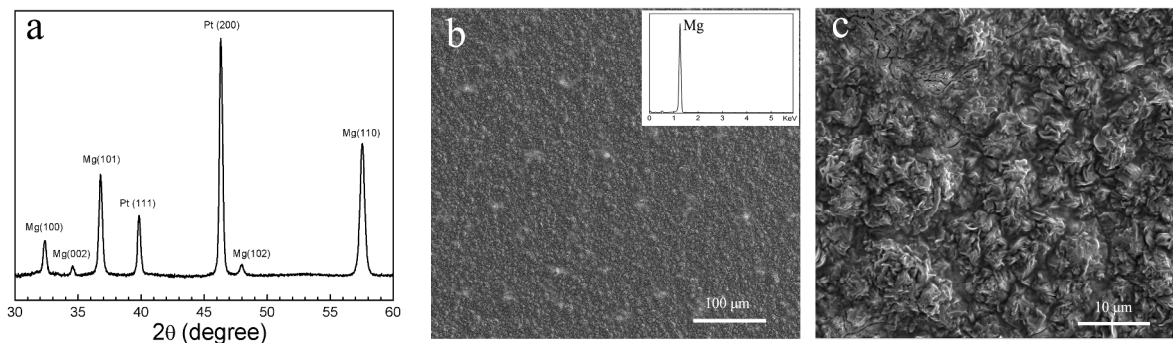


Figure 7: (a) XRD diffraction patterns of Mg deposited on Pt and (b,c) typical SEM image of the deposited Mg showing non-dendritic morphology. The inset in (b) is the EDS spectrum showing 100% Mg deposition.

Mg metal deposited from the $\text{MgCl}_2\text{-AlEtCl}_2/\text{DME}$ electrolyte was analyzed with XRD, SEM and EDX. The deposition rate was 1 mA/cm^2 and a piece of Pt foil was used as the deposition substrate. Figure 7a shows the XRD diffraction pattern collected from the sample, suggesting successful deposition of Mg metal. Figure 7b and c are the SEM images, showing that the deposited Mg metal is smooth, uniform and free of dendritic structures. The deposited Mg grains are in rock shape with the sizes of $5\sim 10 \mu\text{m}$. Such uniform Mg deposition is very important for practical uses. EDS measurement (Figure 7b, inset) further confirmed pure magnesium without impurities.

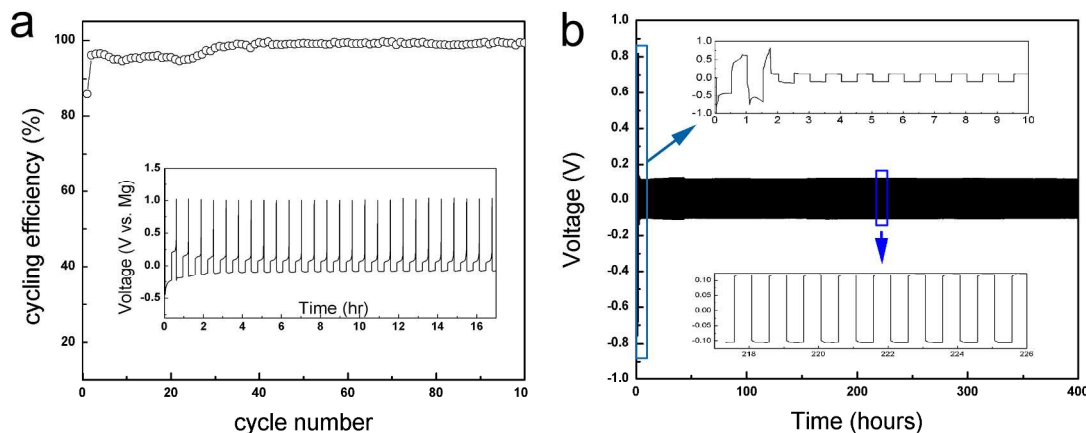


Figure 8: Cycling behavior of the 0.4M $\text{MgCl}_2\text{-AlEtCl}_2/\text{DME}$ electrolyte (a) coulombic efficiency of coin cells assembled with Cu disk positive electrode and Mg disk negative electrode, measured at a current density of 0.5 mA/cm^2 . The inset is the initial 25 cycles of Mg deposition/stripping; (b) voltage profile of Mg-Mg symmetric cells tested with a high current density of 8.0 mA/cm^2 for 400 cycles, 30min for charging and 30min for discharging, the anode and cathode disk are both Mg metal.

The Mg deposition and stripping behavior of the $0.4\text{M MgCl}_2\text{-AlEtCl}_2/\text{DME}$ electrolyte was further evaluated via chronopotentiometry using coin cells, which contains a Cu positive electrode and an Mg negative electrode. The coulombic efficiency (to a final stripping potential of 1.0V) for the first cycle was $\sim 85\%$ but quickly increased to $> 95\%$ for the second and subsequent cycles (Figure 8a). Overall, the stabilized cycling efficiency was $\sim 99\%$. Despite the high initial overpotential for activation, the cycling for over hundreds of cycles had average cell overpotential of $\sim 100\text{mV}$. In another set of experiment to evaluate this electrolyte, we assembled Mg//Mg symmetric coin cells and tested these cells via chronopotentiometry at a high current density of 8.0 mA/cm^2 , with the charging and discharging time both set at 30min. Figure 8b shows typical voltage profiles for 400 cycles. Similar high overpotential of $\sim 600\text{mV}$ was observed for the initial few cycles (~ 3 cycles) but the overpotential for stabilized cycling was $\sim 100 \text{ mV}$ and was very stable, with no obvious voltage spike or appreciable increase over continuous cycles.

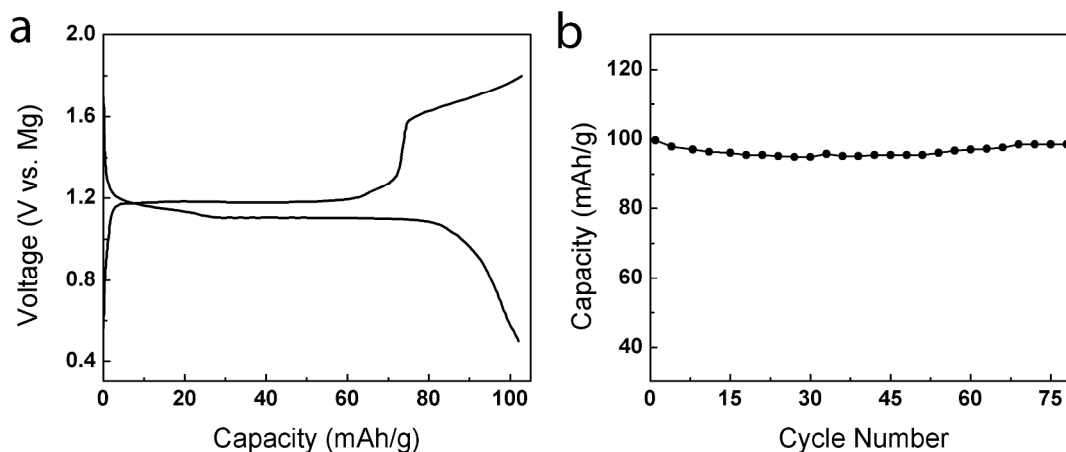


Figure 9 Galvanostatic cycling of Mo_6S_8 cathode in the electrolyte prepared by 0.4M $\text{MgCl}_2\text{-AlEtCl}_2$ in DME at a rate of $c/10$: (a) typical charge-discharge profile and (b) cyclic stability for 75 cycles. The battery tests were conducted at room temperature.

To confirm the compatibility of electrolytes containing the $[\text{Mg}_2(\mu\text{-Cl})_2(\text{DME})_4]^{2+}$ complex with Mg^{2+} ion intercalation cathodes, prototype coin cells were assembled using Mg disk anode and *Chevrel* phase Mo_6S_8 cathode and were tested. The typical charge-discharge profiles at a rate of $C/10$ are shown in Figure 9a. The typical reversible capacity was ~ 100 mAh/g and the voltage profile is comparable to those observed when cycling in the APC electrolytes (Figure 9a).⁵ The cycling tests suggest minimal capacity fade upon cycles (Figure 9b). The well-defined charge-discharge profiles suggest a highly reversible intercalating behavior of Mg^{2+} ions in the electrolyte into Mo_6S_8 cathodes. These results clearly suggest that $[\text{Mg}_2(\mu\text{-Cl})_2(\text{DME})_4]^{2+}$ complex based electrolyte can be incorporated into rechargeable Mg batteries.

Conclusions

In summary, we established the formulation and first identification of the unique cation complex $[\text{Mg}_2(\mu\text{-Cl})_2(\text{DME})_4]^{2+}$ for highly active Mg electrolytes. This cation complex can be formulated in DME by dehalodimerization of non-nucleophilic MgCl_2 through reacting with

either a Mg salt $\text{Mg}(\text{TFSI})_2$ or a Lewis acid salt (AlEtCl_2 or AlCl_3) and its structure was extensively studied using single-crystal XRD, Raman and NMR characterizations. The feasibility of these electrolytes for practical Mg batteries was evidenced by their outstanding Mg deposition activity and reversibility (up to 100% stable cycling efficiency), high anodic stability (up to 3.5V) and ionic conductivity. The new active species identified here and its synthesis and understanding could provide new approaches for rational formulation of Mg electrolytes and design of high energy density magnesium batteries.

ASSOCIATED CONTENT

Supporting information

Electronic Supplementary Information (ESI) available: Detailed synthesis methods, full details of single crystal X-ray structure refinement and additional supporting figures.

AUTHOR INFORMATION

Corresponding Author

guosheng.li@pnnl.gov

Notes

The authors declare no competing financial interest.

Acknowledgement:

We would like to gratefully acknowledge the support from the U.S. Department of Energy (DOE) Office of Electricity Delivery and Energy Reliability under Contract No. 57558 and the Laboratory-Directed Research and Development Program of Pacific Northwest National

Laboratory (PNNL). NMR, Raman, and SEM characterizations were performed in the Environmental Molecular Sciences Laboratory, a national scientific user facility sponsored by DOE's Office of Biological and Environmental Research, located at PNNL. PNNL is a multiprogram laboratory operated by Battelle Memorial Institute for the DOE under Contract DE-AC05-76RL01830.

Reference:

1. D. Aurbach, Z. Lu, A. Schechter, Y. Gofer, H. Gizbar, R. Turgeman, Y. Cohen, M. Moshkovich and E. Levi, *Nature*, 2000, **407**, 724-727.
2. H. D. Yoo, I. Shterenberg, Y. Gofer, G. Gershinsky, N. Pour and D. Aurbach, *Energ Environ Sci*, 2013, **6**, 2265-2279.
3. P. Saha, M. K. Datta, O. I. Velikokhatnyi, A. Manivannan, D. Alman and P. N. Kumta, *Prog Mater Sci*, 2014, **66**, 1-86.
4. Y. W. Cheng, Y. Y. Shao, J. G. Zhang, V. L. Sprenkle, J. Liu and G. S. Li, *Chem Commun*, 2014, **50**, 9644-9646.
5. Y. Cheng, L. R. Parent, Y. Shao, C. Wang, V. L. Sprenkle, G. Li and J. Liu, *Chemistry of Materials*, 2014, **26**, 4904-4907.
6. Y. L. Liang, R. J. Feng, S. Q. Yang, H. Ma, J. Liang and J. Chen, *Adv Mater*, 2011, **23**, 640-+.
7. Y. N. NuLi, Y. P. Zheng, F. Wang, J. Yang, A. I. Minett, J. L. Wang and J. Chen, *Electrochem Commun*, 2011, **13**, 1143-1146.
8. R. G. Zhang, X. Q. Yu, K. W. Nam, C. Ling, T. S. Arthur, W. Song, A. M. Knapp, S. N. Ehrlich, X. Q. Yang and M. Matsui, *Electrochem Commun*, 2012, **23**, 110-113.
9. Y. Y. Shao, T. B. Liu, G. S. Li, M. Gu, Z. M. Nie, M. Engelhard, J. Xiao, D. P. Lv, C. M. Wang, J. G. Zhang and J. Liu, *Sci Rep-Uk*, 2013, **3**.

10. N. Pour, Y. Gofer, D. T. Major and D. Aurbach, *J Am Chem Soc*, 2011, **133**, 6270-6278.
11. J. Muldoon, C. B. Bucur, A. G. Oliver, T. Sugimoto, M. Matsui, H. S. Kim, G. D. Allred, J. Zajicek and Y. Kotani, *Energ Environ Sci*, 2012, **5**, 5941-5950.
12. Y. S. Guo, F. Zhang, J. Yang, F. F. Wang, Y. N. NuLi and S. I. Hirano, *Energ Environ Sci*, 2012, **5**, 9100-9106.
13. T. B. Liu, Y. Y. Shao, G. S. Li, M. Gu, J. Z. Hu, S. C. Xu, Z. M. Nie, X. L. Chen, C. M. Wang and J. Liu, *J Mater Chem A*, 2014, **2**, 3430-3438.
14. Z. Zhao-Karger, J. E. Mueller, X. Y. Zhao, O. Fuhr, T. Jacob and M. Fichtner, *Rsc Adv*, 2014, **4**, 26924-26927.
15. R. E. Doe, R. Han, J. Hwang, A. J. Gmitter, I. Shterenberg, H. D. Yoo, N. Pour and D. Aurbach, *Chem Commun*, 2014, **50**, 243-245.
16. S. Yagi, A. Tanaka, Y. Ichikawa, T. Ichitsubo and E. Matsubara, *J Electrochem Soc*, 2013, **160**, C83-C88.
17. Y. W. Cheng, T. B. Liu, Y. Y. Shao, M. H. Engelhard, J. Liu and G. S. Li, *J Mater Chem A*, 2014, **2**, 2473-2477.
18. D. P. Lv, T. Xu, P. Saha, M. K. Datta, M. L. Gordin, A. Manivannan, P. N. Kumta and D. H. Wang, *J Electrochem Soc*, 2013, **160**, A351-A355.
19. N. Singh, T. S. Arthur, C. Ling, M. Matsui and F. Mizuno, *Chemical Communications*, 2013, **49**, 149-151.
20. Y. Y. Shao, M. Gu, X. L. Li, Z. M. Nie, P. J. Zuo, G. S. Li, T. B. Liu, J. Xiao, Y. W. Cheng, C. M. Wang, J. G. Zhang and J. Liu, *Nano Lett*, 2014, **14**, 255-260.
21. T. S. Arthur, N. Singh and M. Matsui, *Electrochem Commun*, 2012, **16**, 103-106.
22. J. M. Tarascon and M. Armand, *Nature*, 2001, **414**, 359-367.

23. M. C. Kroon, W. Buijs, C. J. Peters and G. J. Witkamp, *Green Chem*, 2006, **8**, 241-245.
24. Z. Lu, A. Schechter, M. Moshkovich and D. Aurbach, *J Electroanal Chem*, 1999, **466**, 203-217.
25. C. Liao, B. K. Guo, D. E. Jiang, R. Custelcean, S. M. Mahurin, X. G. Sun and S. Dai, *J Mater Chem A*, 2014, **2**, 581-584.
26. O. Mizrahi, N. Amir, E. Pollak, O. Chusid, V. Marks, H. Gottlieb, L. Larush, E. Zinigrad and D. Aurbach, *J Electrochem Soc*, 2008, **155**, A103-A109.
27. T. D. Gregory, R. J. Hoffman and R. C. Winterton, *J Electrochem Soc*, 1990, **137**, 775-780.
28. D. Lv, D. Tang, Y. Duan, M. L. Gordin, F. Dai, P. Zhu, J. Song, A. Manivannan and D. Wang, *J Mater Chem A*, 2014, **2**, 15488-15494.
29. D. Aurbach, A. Schechter, M. Moshkovich and Y. Cohen, *J Electrochem Soc*, 2001, **148**, A1004-A1014.
30. F. F. Wang, Y. S. Guo, J. Yang, Y. Nuli and S. Hirano, *Chem Commun*, 2012, **48**, 10763-10765.
31. H. S. Kim, T. S. Arthur, G. D. Allred, J. Zajicek, J. G. Newman, A. E. Rodnyansky, A. G. Oliver, W. C. Boggess and J. Muldoon, *Nat Commun*, 2011, **2**.
32. R. E. Doe, G. H. Lan, R. E. Jilek, and J. H. Hwang, US20130252114, 2013.
33. S. Y. Ha, Y. W. Lee, S. W. Woo, B. Koo, J. S. Kim, J. Cho, K. T. Lee and N. S. Choi, *Acs Appl Mater Inter*, 2014, **6**, 4063-4073.
34. J. Muldoon and C. B. Bucur, US8722242 B2, 2011.
35. Y. Gofar, O. Chusid, H. Gizbar, Y. Viestfrid, H. E. Gottlieb, V. Marks and D. Aurbach, *Electrochemical and Solid-State Letters*, 2006, **9**, A257-A260.

36. M. C. Lefebvre and B. E. Conway, *J Electroanal Chem*, 1998, **448**, 217-227.
37. A. G. Potapov, V. V. Terskikh, G. D. Bukatov and V. A. Zakharov, *J Mol Catal a-Chem*, 2000, **158**, 457-460.
38. C. E. Keller and W. R. Carper, *Inorg Chim Acta*, 1993, **210**, 203-208.
39. P. H. Heubel and A. I. Popov, *J Solution Chem*, 1979, **8**, 283-291.
40. H. Gizbar, Y. Vestfrid, O. Chusid, Y. Gofer, H. E. Gottlieb, V. Marks and D. Aurbach, *Organometallics*, 2004, **23**, 3826-3831.

Graphical Abstract

